Electronic Supplementary Material (ESI) for RSC Advances.

Supporting Information

Structures of 4-Substituented Thioanisole Radical Cations Studied by Time-resolved Resonance Raman Spectroscopy during Pulse Radiolysis and Theoretical Calculations

Sachiko Tojo, Mamoru Fujitsuka, and Tetsuro Majima**

The Institute of Scientific and Industrial Research (SANKEN), Osaka University, Mihogaoka 8-1, Ibaraki, Osaka 567-0047, Japan,

E-mail: fuji@sanken.osaka-u.ac.jp; majima@sanken.osaka-u.ac.jp

Raman spectra of conformers in the neutral state.

Here, conformers of the compounds in this study were studied by DFT calculations. To find conformers, initial structures, which were generated by systematically changing dihedral angle(s) formed by benzene rings and substituent(s) ($\phi(C_2C_1S_7C_8)$ and $\phi(C_3C_4X_9Y_{10})$ in Chart S1), were subjected to optimization. For MTPM, MTPA, and MTA, 11 initial structures were subjected to optimization, while 4 structures were used for optimization of MTB and MTT. For optimization at (U)B3LYP/6-311+g(d,p) level using Gaussian 09 package, ultrafine grid and tight convergence were employed, and absence of imaginary frequency was confirmed. Following Tables summarized dihedral angle(s) (ϕ) and sum of electronic and zero-point energies of the optimized structures. In these table, conformers are distinguished by small alphabet (a, b, c…) and symmetrical conformers are ignored.

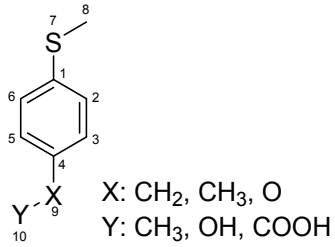

Chart S1.

Table S1. Conformers of MTPM in neutral and radical cation state estimated by DFT calculations at (U)B3LYP/6-311+G(d,p) level.[a]

	Charge	$\phi(C_2C_1S_7C_8)$	$\phi(C_3C_4X_9Y_{10})$	sum of electronic and zero-point energies (eV)
MTPMa	0	0.7	153.4	-21340.437
MTPMb	0	1.5	-15.2	-21340.444
MTPMc	0	89.8	-12.2	-21340.455
MTPMd	1	0.0 (0.0)	0.0 (0.0)	-21333.063

MTPMe	1	0.0 (0.0)	180.0 (180.0)	-21333.061

[a] Numbers in parentheses are estimated at UBP86/TZVP.

Table S2. Conformers of MTPA in neutral and radical cation state estimated by DFT calculations at (U)B3LYP/6-311+G(d,p) level.[a]

	Charge	$\phi(C_2C_1S_7C_8)$	$\phi(C_3C_4X_9Y_{10})$	sum of electronic and zero-point energies (eV)
MTPAa	0	1.5	-106.5	-24426.053
MTPAb	0	2.6	-71.8	-24426.053
MTPAc	0	80.8	75.4	-24426.039
MTPAd	0	82.1	71.0	-24426.030
MTPAe	1	0.2 (-[b])	-121.4 (-[b])	-24418.467
MTPAf	1	0.3 (0.3)	-57.5 (-81.0)	-24418.477

[a] Numbers in parentheses are estimated at UBP86/TZVP. [b] Related structure did not obtained at the UBP86/TZVP level with Gaussian 09.

Table S3. Conformers of MTB in neutral and radical cation state estimated by DFT calculations at (U)B3LYP/6-311+g(d,p) level.[a]

	Charge	$\phi(C_2C_1S_7C_8)$	$\phi(C_3C_4X_9Y_{10})$	sum of electronic and zero-point energies (eV)
MTBa	0	0.0	-	-18224.146
MTBb	0	89.0	-	-18224.127
MTBc	1	0.0 (0.0)	-	-18216.412

[a] Numbers in parentheses are estimated at UBP86/TZVP.

Table S4. Conformers of MTT in neutral and radical cation state estimated by DFT calculations at (U)B3LYP/6-311+G(d,p) level.[a]

	Charge	$\phi(C_2C_1S_7C_8)$	$\phi(C_3C_4X_9Y_{10})$	sum of electronic and zero-point energies (eV)
MTTa	0	0.0	-	-19293.568
MTTb	0	88.9	-	-19293.562
MTTc	1	0.0 (0.0)	-	-19286.092

[a] Numbers in parentheses are estimated at UBP86/TZVP.

Table S5. Conformers of MTA in neutral and radical cation state estimated by DFT calculations at (U)B3LYP/6-311+G(d,p) level.[a]

	Charge	$\phi(C_2C_1S_7C_8)$	$\phi(C_3C_4X_9Y_{10})$	sum of electronic and zero-point energies (eV)
MTAa	0	0.0	0.0	-21340.495
MTAb	0	87.2	179.5	-21340.522
MTAc	1	0.0 (0.0)	0.0 (0.0)	-21333.331
MTAd	1	0.0 (0.0)	180.0 (180.0)	-21333.345

[a] Numbers in parentheses are estimated at UBP86/TZVP.

In Figure S1, Raman spectrum of MTPM is compared with theoretically estimated Raman spectra of conformers. It should be noted, that the calculated wavenumbers were scaled by using a factor of 0.97. Raman peak positions depend on the structures: For example, ring stretching mode of MTPMa, -b, and -c located at 1597, 1598, and 1592 cm^{-1}. These are difficult to distinguish with the present spectral resolution. Furthermore, small energy difference between these conformer (18 meV) indicates that the

all conformers are possible in the room temperature experiments. Thus, the present spectrum seems to sum of these conformers.

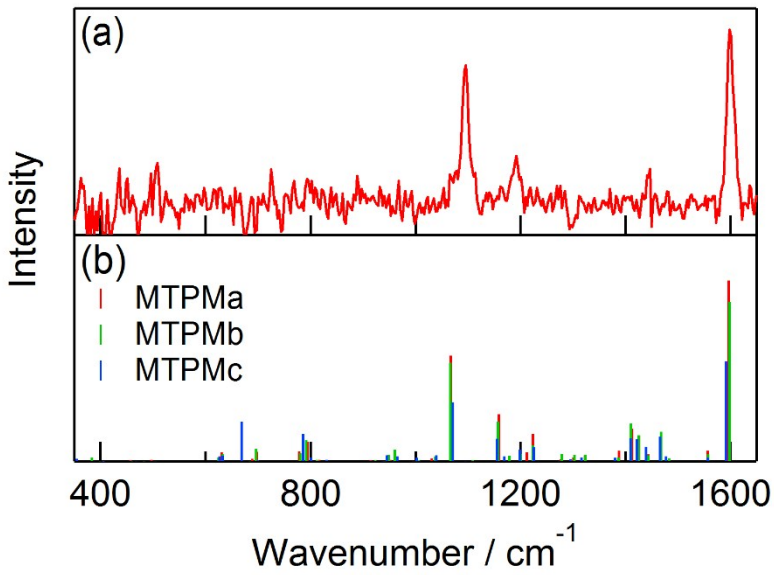

Figure S1. (a) Raman spectrum of MTPM in DCE. (b) Theoretically estimated Raman spectra of conformers at B3LYP/6-311+G(d,p) level.

Table S6. Observed Raman peaks of $ArSCH_3$.

Mode assignments	MTPM	MTPA	MTT	MTB	MTA
C=C str/r	1599 vs[a]	1599 vs	1601 vs	1581 vs	1596 vs, 1570 s
CH bend/OCH_3					1493 w
CH bend/r				1482, 1438 w	
CH bend/SCH_3 CH bend/OCH_3					1427 w
C_r-O str/C_rOCH_3					1300 m
CH bend/CH_3			1377 w		
C_r-C str/C_rCH_3			1211 vw		
CH bend/r	1192 m	1192 m	1184 m	1159 w	1192 s
C_r-S str/C_rSCH_3	1096 s	1093 s	1096 vs	1090 s	1096 vs

CH bend/r			
Deformation/r		999 s	
CH bend/r CH bend/SCH_3			
Breathing/r	794 w		800 m
S-CH_3 str	721 vw		
C_r-S str/C_rSCH_3		690 w	
Deformation/r	653 w		

[a] Intensity description: vs = very strong, s = strong, m = medium, w = weak, vw = very weak.
Abbreviations used in table: str: stretching, r: ring.

Time-resolved Raman Spectra of MTPM$^{\bullet+}$

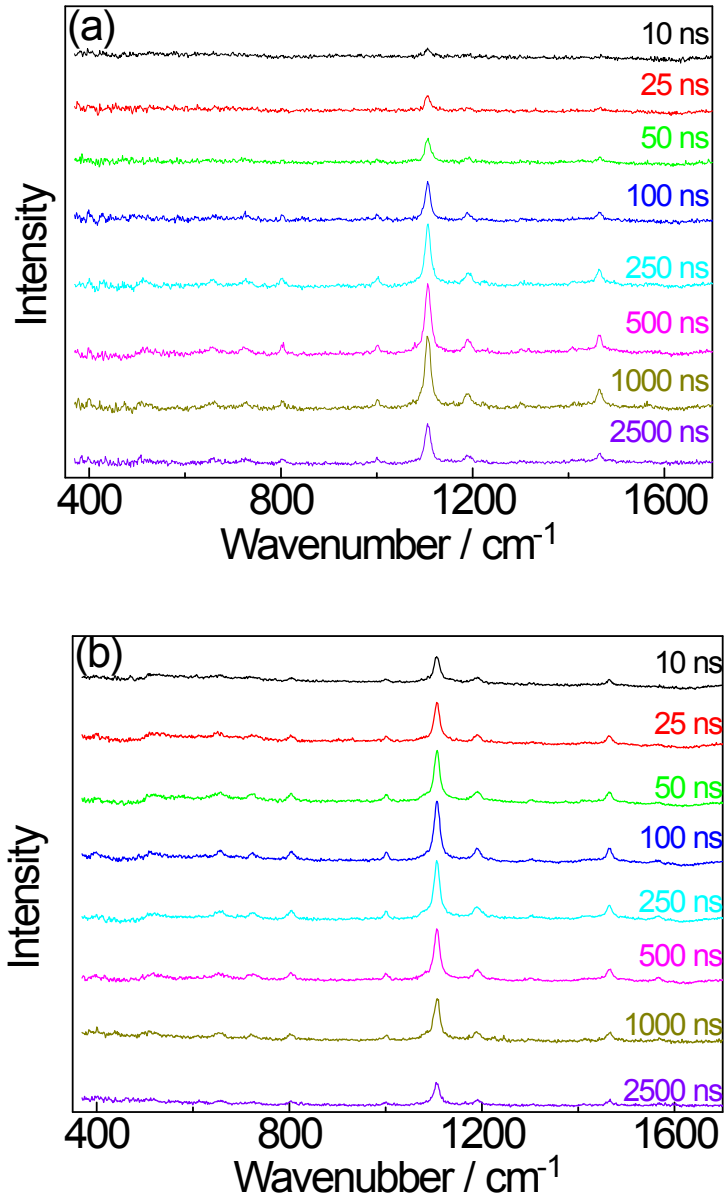

Figure S2. ns-TR^3 spectra observed at various time delays excited at 532 nm after an electron pulse during the pulse radiolysis of MTPM (a)0.5 mM and (b)5 mM in N_2O-saturated aqueous solution (pH 7) containing NaBr (100 mM) excited at 532 nm.

Raman Spectrum of $Br_2^{\bullet-}$

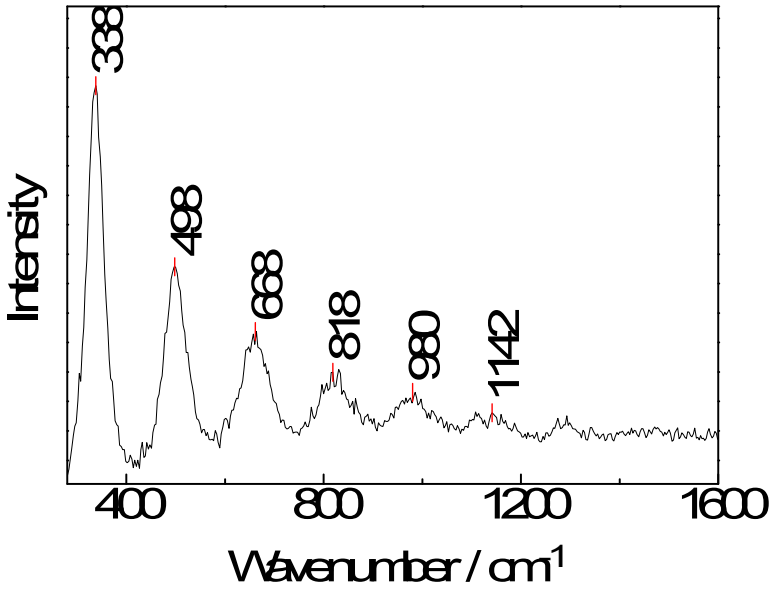

Figure S3. ns-TR[3] spectra of $Br_2^{\bullet-}$ observed at 500 ns after an electron pulse during the pulse radiolysis of N_2O-saturated aqueous solution containing NaBr (100 mM) excited at 355 nm.

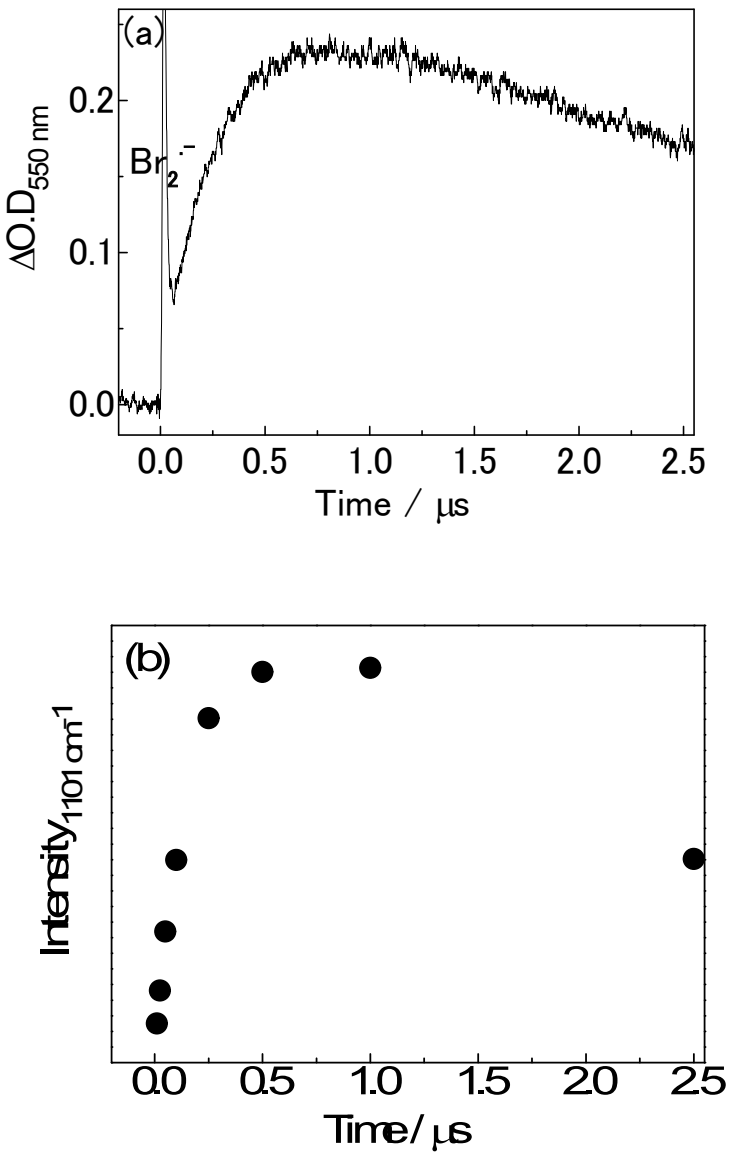

Figure S4. Time profiles of ns-TA at 550 nm showing the formation of $MTPM^{\bullet+}$ (A) and ns-TR[3] at 1101 cm^{-1} (B) after an electron pulse during the pulse radiolysis of MTPM with 0.5 mM in N_2O-saturated aqueous solution (pH 7) containing NaBr (100 mM).

Assignments of resonance Raman peaks.

In the case of Raman spectrum measured under non-resonance condition, Raman peaks can be reasonably simulated by Gaussian 09 package. However, Gaussian 09 does not support resonance

Raman. At present, theoretical calculation of resonance Raman spectrum of the open shell system can be performed by NWChem which includes TD-DFT linear response module for unrestricted DFT calculation developed by Aquino and Schatz, recently. Thus, we used NWChem 6.6, to which available patches are applied. For calculation, becke88 perdew86 exchange-correlation functional and TZVP basis set were employed after their study. As in the case of neutral state, observed spectra of radical cations will be sum of those of several conformers because of small difference in the sum of electronic and zero-point energies (Table S1-S5).

TR^3 spectrum of MTB radical cation and theoretical calculation results are indicated in Figure S5 (Factor for wavenumber: 1.00). For comparison purpose, theoretically estimated non-resonance spectrum (Gaussian 09) is also indicated. Although NWChem underestimated intensity of a peak around 400 cm^{-1}, other peaks are reasonably simulated. It can be seen that the present theory (BP86) and basis set underestimate wavenumber by 2-3%.

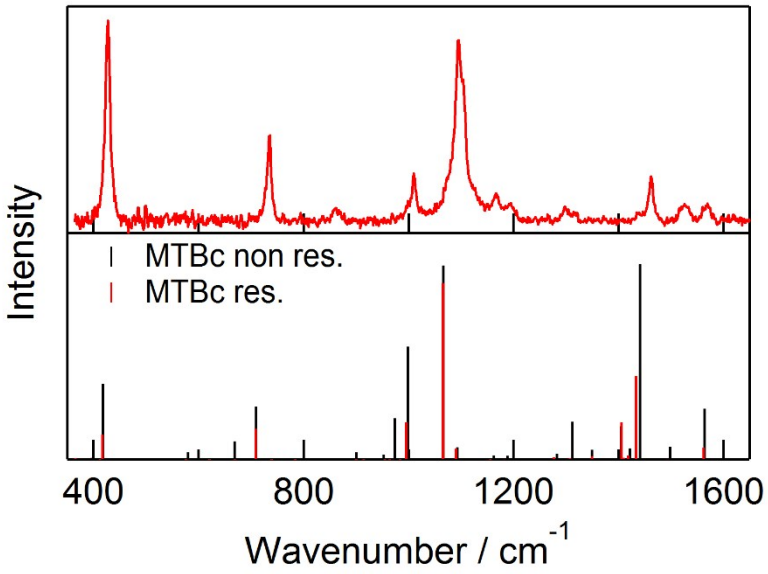

Figure S5. (Upper panel) TR^3 spectrum of MTB with 1 mM in N_2O-saturated aqueous solution (pH 7) containing NaBr (100 mM) during pulse radiolysis. (Lower panel) Theoretically estimated Raman spectra of TMB radical cation under resonance and non-resonance conditions.

Table S7. Observed Raman peaks of $ArSCH_3^{\bullet+}$.

Mode assignments	$MTPM^{\bullet+}$	$MTPA^{\bullet+}$	$MTT^{\bullet+}$	$MTB^{\bullet+}$	$MTA^{\bullet+}$
C=C str/r	-	1580 vw[a]	-	1570, 1527 vw	1604 s
CH bend/OCH_3					1498 vw
CH bend/r CH bend/SCH_3	1475 m	1470 m	1475 m	1462 w	1457 vw
CH bend/SCH_3 CH bend/OCH_3					1424 vw
C-O str/OCH_3					1317 vw
CH bend/CH_3					
C_r-C str/C_rCH_3			1230 w		
C_r-C str/C_rCH_2OH	1294 vw				
CH bend/CH_2		1265 w			
CH bend/CH_2COOH		1193 m			
CH bend/r	1183 m		1199 vw	1104 s	
C_r-S str/C_rSCH_3 CH bend/r	1101 vs	1103 vs	1107 vs	1095 vs	1119 vs
CH bend/r CH bend/SCH_3	998 w	1002 m	1001 w	1009 m	998 w
Breathing/r	803 w	813 vw	802 m		804 w
S-CH_3 str	721 w	719 vw	721 vw	737 s	719 w
C_r-S str/C_rSCH_3	657 w	680 vw	641 m		664 w
Deformation/r	524 w	459 m	408 m	428 vs	503 w

[a] Intensity description: vs = very strong, s = strong, m = medium, w = weak, vw = very weak.
Abbreviations used in table: str: stretching, r: ring.

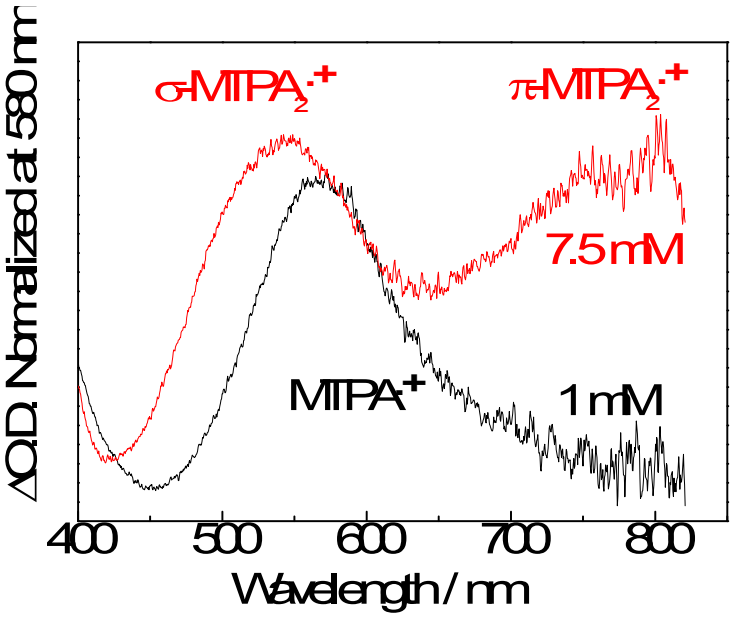

Figure S6. ns-TA spectra observed at 500 ns after an electron pulse during the pulse radiolysis of MTPA with 1 mM (black) and 7.5 mM (red) in N_2O-saturated aqueous solution (pH 7) containing NaBr (100 mM). The optical densities of two spectra are normalized at 580 nm.

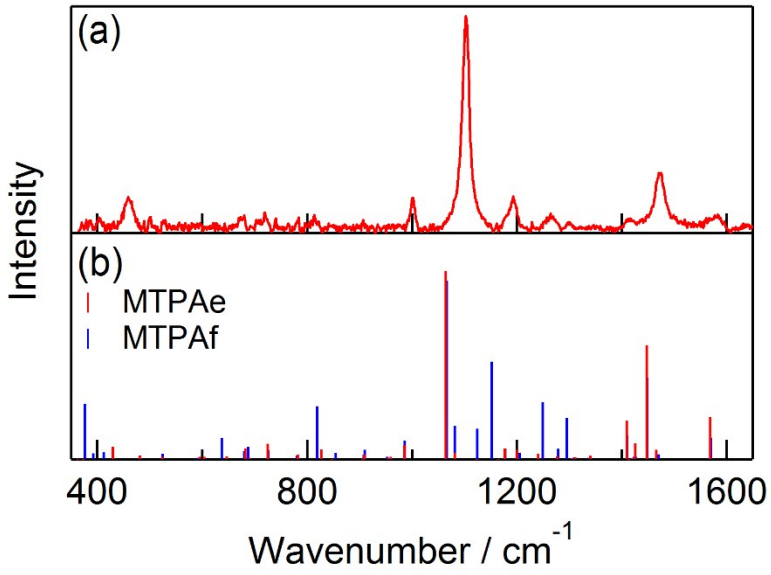

Figure S7. (a) ns-TR[3] spectrum observed at 500 ns after an 8-ns electron pulse during the pulse radiolysis of MTPA (1 mM) in N_2O-saturated aqueous solution containing NaBr (100 mM). Probe: 532

nm. (b) Raman peaks of two conformers of $MTPM^{\bullet+}$ (Table S2) calculated by TDDFT at UBP86/TZVP level.

Table S8. Bond lengths (Å) of $ArSCH_3$ and $ArSCH_3^{\bullet+}$ by the DFT calculation at the UB3LYP/6-311+G(d,p) level.[a]

Bond	MTPM	$MTPM^{\bullet+}$	MTPA	$MTPA^{\bullet+}$	MTT	$MTT^{\bullet+}$	MTB	$MTB^{\bullet+}$	MTA	$MTA^{\bullet+}$
C_1-S	1.798	1.720	1.781	1.721	1.784	1.719	1.800	1.719	1.787	1.723
C_1-C_2	1.398	1.428	1.397	1.419	1.396	1.420	1.399	1.428	1.397	1.427
C_2-C_3	1.392	1.372	1.395	1.374	1.397	1.374	1.394	1.378	1.394	1.371
C_3-C_4	1.399	1.419	1.393	1.419	1.394	1.420	1.394	1.404	1.398	1.418
C_4-C_5	1.397	1.414	1.400	1.412	1.402	1.415	1.394	1.410	1.397	1.425
C_5-C_6	1.391	1.376	1.388	1.375	1.388	1.374	1.394	1.377	1.390	1.368
C_6-C_1	1.399	1.419	1.403	1.426	1.403	1.427	1.399	1.420	1.401	1.421
C_4-C_9	1.516	1.497	-	-	-	-	-	-	-	-
C_4-O	-	-	-	-	-	-	-	-	1.367	1.317

[a] Bond length of the most stable comformers ($MTPMd^{\bullet+}$, $MTPAf^{\bullet+}$, $MTTc^{\bullet+}$. $MTBc^{\bullet+}$, and $MTAd^{\bullet+}$, See Table S1-S5) are indicated.

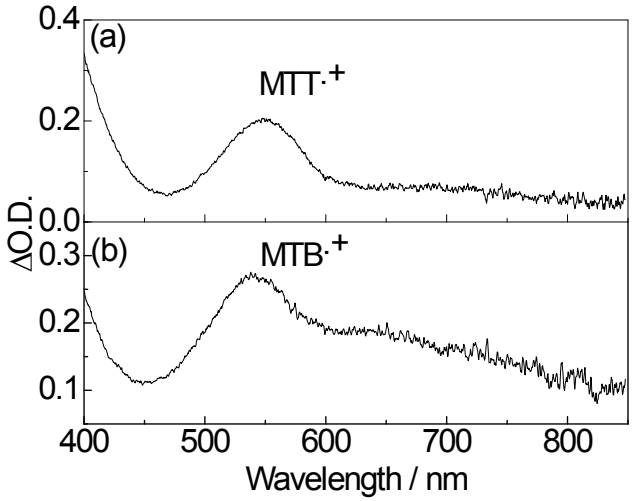

Figure S8. ns-TA spectra observed at 500 ns after an electron pulse during the pulse radiolysis of (a) MTT and (b) MTB with 1 mM in N_2O-saturated aqueous solution (pH 7) containing NaBr (100 mM).

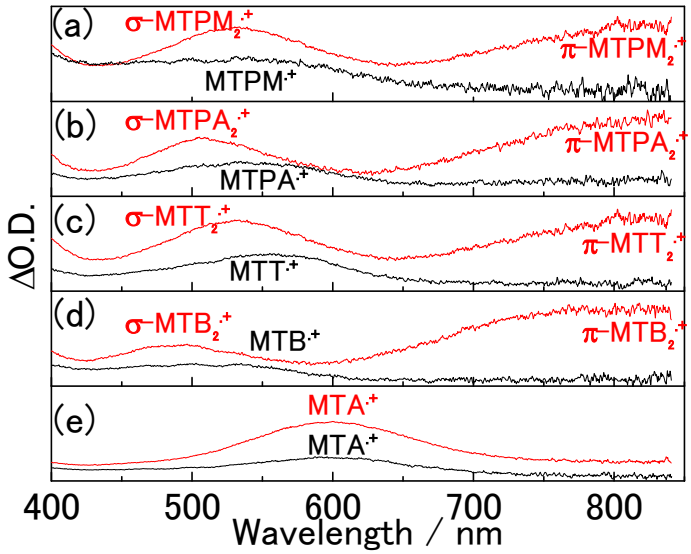

Figure S9. ns-TA spectra observed at 50 ns after an electron pulse during the pulse radiolysis of $ArSCH_3$ with 1 mM (black) and 50 mM (red) in benzonitrile. (a) MTPM, (b) MTPA, (c) MTT, (d) MTB and (e) MTA.

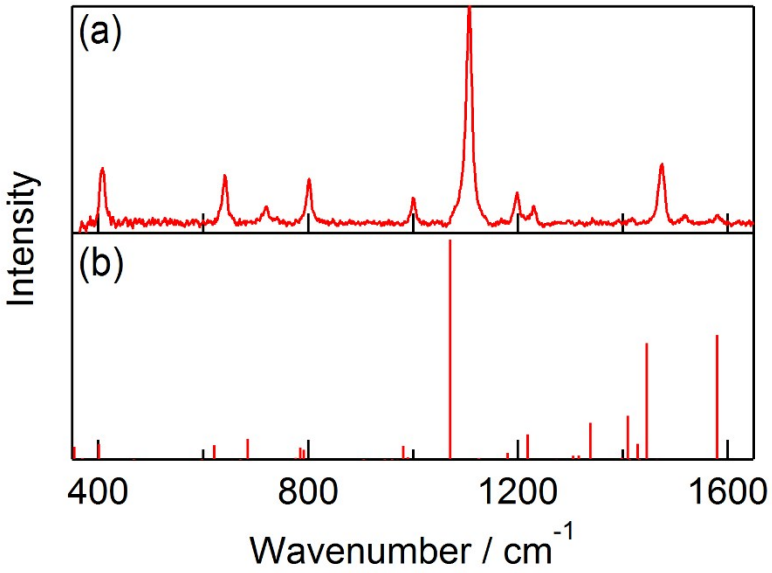

Figure S10. (a) ns-TR[3] spectrum observed at 500 ns after an 8-ns electron pulse during the pulse radiolysis of MTT (1 mM) in N_2O-saturated aqueous solution containing NaBr (100 mM). Probe: 532 nm. (b) Raman peaks of $MTT^{\bullet+}$ calculated by TDDFT at UBP86/TZVP level.

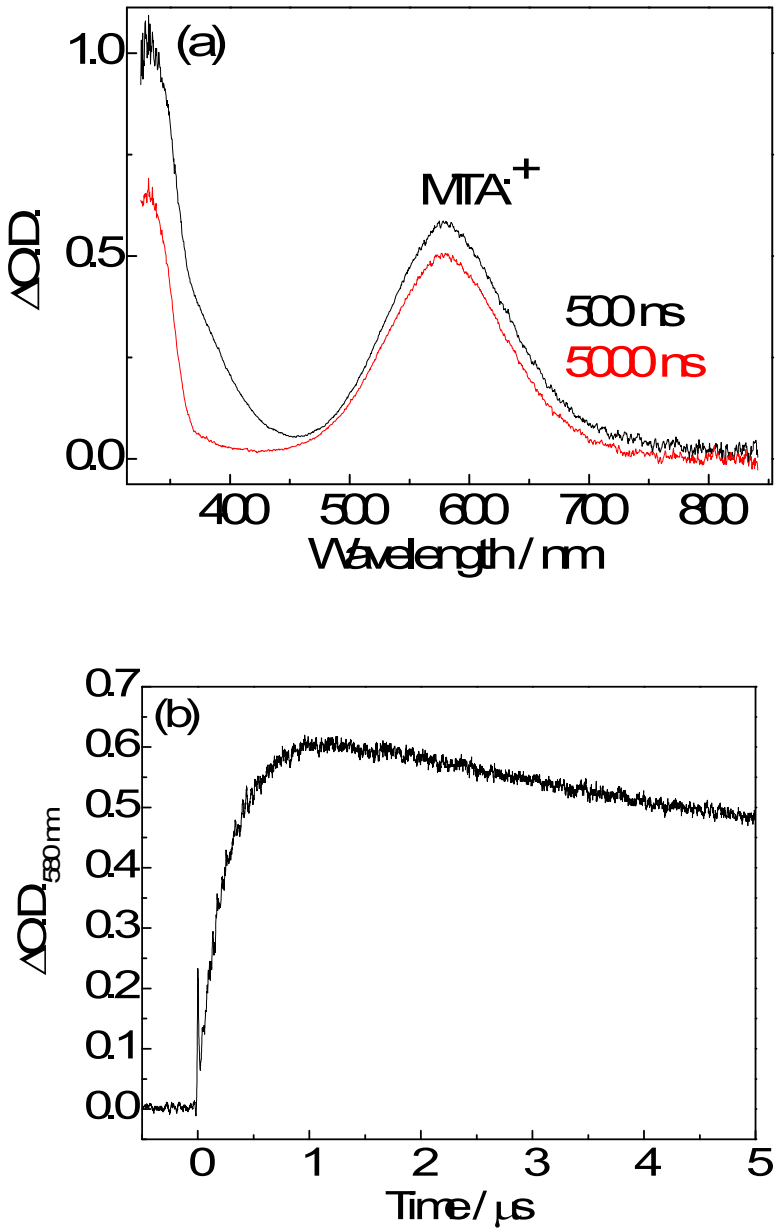

Figure S11. (a) ns-TA spectra observed at 500 (black) and 5000 (red) ns after an electron pulse during the pulse radiolysis of MTA 1 mM with in N_2O-saturated aqueous solution (pH 7) containing NaBr (100 mM). (b) Time profiles of ns-TA at 580 nm showing the formation of $MTA^{\bullet+}$ after an electron pulse during the pulse radiolysis of MTA 1 mM with in N_2O-saturated aqueous solution (pH 7) containing NaBr (100 mM).

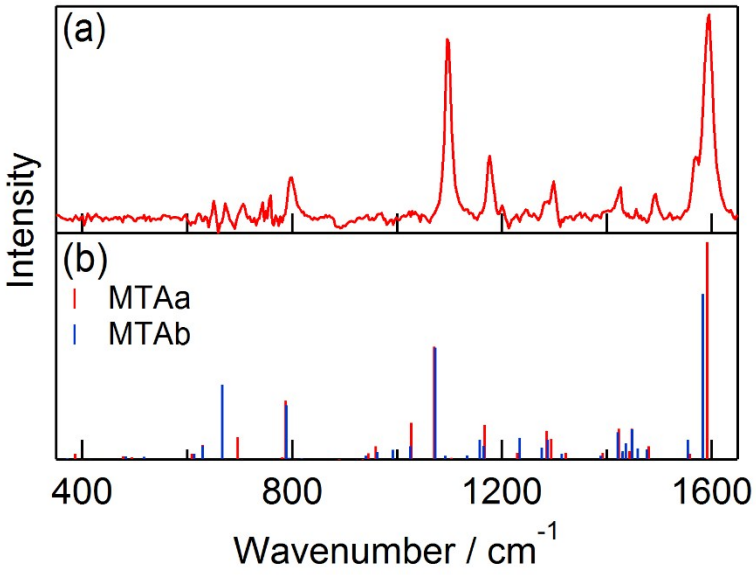

Figure S12. (a) Raman spectrum of MTA in DCE. (b) Theoretically estimated Raman spectra of conformers at B3LYP/6-311+G(d,p) level.

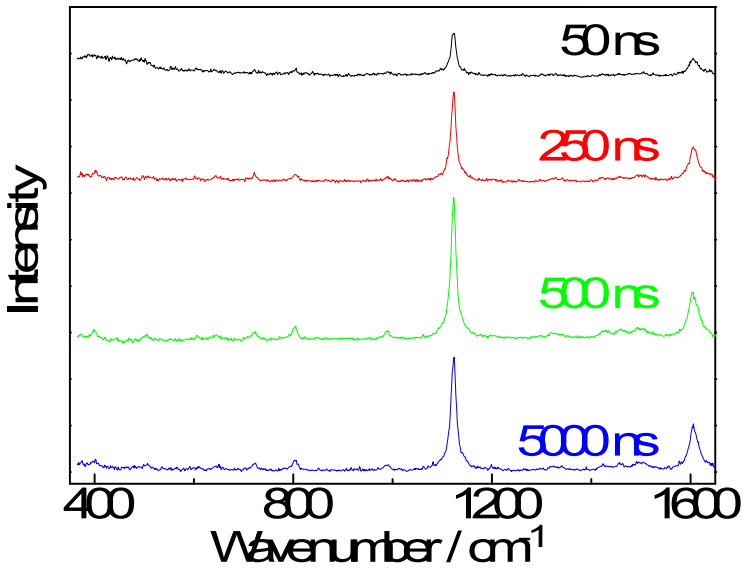

Figure S13. ns-TR^3 spectra observed at various times after an electron pulse during the pulse radiolysis of MTA(1 mM) in N_2O-saturated aqueous solution containing NaBr (100 mM) excited at 532 nm.

Table S9. XYZ coordinate of MTPMa by B3LYP/6-311+G(d,p).

	X	Y	Z
C	-1.02395	-0.24581	-0.02395
C	-0.56095	1.071534	0.010745
C	0.808409	1.331381	-0.01671
C	1.741134	0.29887	-0.09036
C	1.271515	-1.0176	-0.1198
C	-0.08921	-1.28837	-0.08481
S	-2.74556	-0.71635	0.014213
C	-3.62249	0.87697	0.083182
C	3.217556	0.601207	-0.17656
O	3.962865	-0.48668	0.363193
H	-1.25108	1.902693	0.069485
H	1.146923	2.362591	0.024037
H	1.98657	-1.8296	-0.15457
H	-0.43202	-2.31737	-0.1031
H	-4.68259	0.623004	0.10124
H	-3.42005	1.483669	-0.80023
H	-3.37701	1.430166	0.990444
H	3.428506	1.533283	0.366264
H	3.49142	0.766399	-1.22999
H	4.883221	-0.36903	0.11297

Table S10. XYZ coordinate of MTPMb by B3LYP/6-311+G(d,p).

	X	Y	Z
C	1.047572	0.30454	-0.00567
C	0.356376	-0.90692	-0.05457
C	-1.03883	-0.92364	-0.0738

C	-1.77056	0.259613	-0.04215
C	-1.07259	1.471084	0.014758
C	0.31382	1.499163	0.029482
S	2.82614	0.459626	0.019423
C	3.404039	-1.26626	0.011586
C	-3.28007	0.257864	-0.09286
O	-3.77181	-1.04917	0.179646
H	0.888591	-1.84878	-0.07703
H	-1.56766	-1.86727	-0.10595
H	-1.61903	2.40913	0.051611
H	0.833228	2.450187	0.076063
H	4.492355	-1.20714	0.037866
H	3.100593	-1.7859	-0.89789
H	3.0578	-1.80673	0.893223
H	-3.60635	0.593274	-1.08931
H	-3.66532	0.983684	0.638038
H	-4.7165	-1.05383	0.004746

Table S11. XYZ coordinate of MTPMc by B3LYP/6-311+G(d,p).

	X	Y	Z
C	-1.04452	0.070877	-0.31274
C	-0.23534	-1.06546	-0.37214
C	1.145786	-0.95973	-0.22005
C	1.740524	0.284256	-0.01155
C	0.928824	1.42118	0.044454
C	-0.44926	1.320327	-0.1097
S	-2.823	-0.0609	-0.54321
C	-3.36991	-0.33411	1.18722
C	3.23852	0.426191	0.126175

O	3.834173	-0.85339	0.292708
H	-0.68968	-2.03442	-0.54312
H	1.771977	-1.84102	-0.26186
H	1.376253	2.397478	0.207501
H	-1.0698	2.207903	-0.074
H	-4.45613	-0.43057	1.154558
H	-3.10308	0.514002	1.817842
H	-2.93967	-1.25088	1.590347
H	3.458146	1.07854	0.983803
H	3.630606	0.924882	-0.77311
H	4.788219	-0.74558	0.257716

Table S12. XYZ coordinate of MTPMd$^{\bullet+}$ by UB3LYP/6-311+G(d,p).

	X	Y	Z
C	1.044755	0.288198	-0.00018
C	0.344671	-0.94617	-0.00049
C	-1.0306	-0.94996	-0.00045
C	-1.7558	0.263341	-0.00011
C	-1.0572	1.492806	-0.0002
C	0.313829	1.515137	-0.00022
S	2.756393	0.453585	0.00027
C	3.437964	-1.23191	0.000202
C	-3.25192	0.258635	0.000297
O	-3.72924	-1.06071	0.000302
H	0.881672	-1.88484	-0.00084
H	-1.58278	-1.87991	-0.00065
H	-1.60857	2.426361	-0.00024
H	0.848269	2.458028	-0.00024
H	4.519184	-1.09797	0.000285

H	3.136743	-1.76549	-0.90092
H	3.136594	-1.76571	0.901119
H	-3.59127	0.826963	-0.88257
H	-3.59085	0.826884	0.883333
H	-4.69159	-1.05648	0.000821

Table S13. XYZ coordinate of $MTPMe^{\bullet+}$ by UB3LYP/6-311+G(d,p).

	X	Y	Z
C	-1.0233	-0.22692	0.000001
C	-0.56821	1.118078	0.000003
C	0.780712	1.372857	0.000001
C	1.724406	0.314688	-2E-06
C	1.272078	-1.01954	-2E-06
C	-0.07504	-1.2931	0
S	-2.67254	-0.71483	0.000002
C	-3.66158	0.81045	-4E-06
C	3.186348	0.630601	-2E-06
O	3.93469	-0.5549	0.000001
H	-1.27062	1.940009	0.000008
H	1.129643	2.399724	0.000002
H	2.002152	-1.81712	-2E-06
H	-0.42437	-2.31942	0
H	-4.69793	0.474372	-5E-06
H	-3.46719	1.391704	-0.90107
H	-3.46719	1.391705	0.901063
H	3.396013	1.259087	0.882839
H	3.396012	1.259082	-0.88285
H	4.874023	-0.3454	0.000003

Table S14. XYZ coordinate of MTPAa by B3LYP/6-311+G(d,p).

	X	Y	Z
C	1.73675	-0.23593	-0.12118
C	1.193298	1.04964	-0.07571
C	-0.17137	1.240556	-0.29627
C	-1.02228	0.170416	-0.56535
C	-0.46791	-1.11434	-0.60971
C	0.88646	-1.31896	-0.39189
S	3.457977	-0.61848	0.13606
C	4.208894	1.001089	0.491047
C	-2.49392	0.395662	-0.80406
C	-3.39702	-0.03528	0.339502
O	-3.09522	-0.71636	1.283444
O	-4.65781	0.438925	0.154689
H	1.81574	1.910795	0.12773
H	-0.57139	2.249021	-0.25699
H	-1.10456	-1.96944	-0.80979
H	1.290526	-2.32474	-0.42934
H	5.265489	0.796319	0.665894
H	3.78349	1.450993	1.389009
H	4.117663	1.681196	-0.35684
H	-2.83853	-0.15643	-1.68688
H	-2.70385	1.44694	-1.01553
H	-5.19546	0.113381	0.89236

Table S15. XYZ coordinate of MTPAb by B3LYP/6-311+G(d,p).

	X	Y	Z
C	-1.74567	0.321025	0.000383

C	-1.08036	-0.81233	0.478715
C	0.291488	-0.77285	0.717577
C	1.034785	0.385685	0.490117
C	0.361074	1.514421	0.0131
C	-1.00665	1.488885	-0.22999
S	-3.49358	0.400089	-0.33833
C	-4.07527	-1.2899	0.006954
C	2.52018	0.430877	0.748968
C	3.363394	-0.34889	-0.24624
O	2.987249	-1.21941	-0.98605
O	4.663508	0.041914	-0.18105
H	-1.61696	-1.73233	0.668608
H	0.786083	-1.6676	1.079671
H	0.911785	2.431114	-0.17292
H	-1.50352	2.378721	-0.60089
H	-5.14314	-1.27686	-0.21303
H	-3.93509	-1.55758	1.054962
H	-3.58985	-2.01979	-0.64205
H	2.758831	0.011886	1.734519
H	2.886723	1.459374	0.768997
H	5.158548	-0.50994	-0.80537

Table S16. XYZ coordinate of MTPAc by B3LYP/6-311+G(d,p).

	X	Y	Z
C	1.766777	0.347147	-0.18889
C	1.09587	1.194894	0.694587
C	-0.29056	1.323675	0.626706
C	-1.03256	0.609475	-0.31561

C	-0.35351	-0.23299	-1.20137
C	1.030239	-0.35971	-1.14556
S	3.558859	0.214006	-0.12804
C	3.747557	-1.36728	0.78436
C	-2.53287	0.752547	-0.37845
C	-3.30229	-0.42711	0.192267
O	-2.85693	-1.50164	0.497203
O	-4.62157	-0.12281	0.305251
H	1.660218	1.754551	1.430923
H	-0.79698	1.988958	1.3188
H	-0.90979	-0.79399	-1.94475
H	1.545353	-1.00194	-1.85031
H	4.820674	-1.54384	0.871151
H	3.292054	-2.19146	0.235376
H	3.311991	-1.29364	1.780844
H	-2.87297	0.868174	-1.4142
H	-2.86766	1.651938	0.144024
H	-5.06846	-0.91112	0.648949

Table S17. XYZ coordinate of MTPAd by B3LYP/6-311+G(d,p).

	X	Y	Z
C	-1.72223	0.000552	-0.24855
C	-0.98924	-1.05331	0.307884
C	0.350775	-0.88098	0.63796
C	0.993596	0.339698	0.408033
C	0.260233	1.38343	-0.15938
C	-1.08557	1.220378	-0.48473
S	-3.44685	-0.2226	-0.70613

C	-4.26164	0.016641	0.92075
C	2.447574	0.533429	0.762678
C	3.423	-0.21462	-0.13096
O	3.170745	-1.13232	-0.86577
O	4.680915	0.274099	0.024367
H	-1.46966	-2.01073	0.472214
H	0.905794	-1.7107	1.061513
H	0.74112	2.337658	-0.34978
H	-1.64341	2.038638	-0.92427
H	-5.33201	-0.10418	0.747404
H	-4.0702	1.017902	1.307111
H	-3.92867	-0.73345	1.638336
H	2.648842	0.186814	1.783734
H	2.720352	1.590715	0.749214
H	5.265122	-0.25655	-0.53829

Table S18. XYZ coordinate of MTPAe$^{\bullet+}$ by UB3LYP/6-311+G(d,p).

	X	Y	Z
C	1.717174	-0.19645	0.118478
C	1.235099	1.131038	-0.01819
C	-0.1051	1.38306	0.163734
C	-1.01305	0.345288	0.484549
C	-0.52429	-0.97462	0.623097
C	0.809789	-1.24824	0.446965
S	3.354023	-0.67959	-0.0856
C	4.291505	0.820806	-0.5037
C	-2.46718	0.648368	0.672839
C	-3.38276	-0.12917	-0.28135

O	-3.07461	-1.12494	-0.87868
O	-4.58825	0.452278	-0.32929
H	1.905617	1.942568	-0.26558
H	-0.47476	2.396127	0.056043
H	-1.20968	-1.77821	0.856488
H	1.178855	-2.26224	0.550867
H	5.320221	0.484159	-0.62897
H	4.240109	1.542576	0.311388
H	3.930281	1.247538	-1.43933
H	-2.67535	1.714157	0.577435
H	-2.7791	0.359154	1.685833
H	-5.16472	-0.07169	-0.90937

Table S19. XYZ coordinate of MTPAf$^{\bullet+}$ by UB3LYP/6-311+G(d,p).

	X	Y	Z
C	-1.73359	0.311897	-0.00019
C	-1.00391	-0.82085	0.444421
C	0.351492	-0.71851	0.643869
C	1.036714	0.503522	0.414
C	0.302976	1.627464	-0.01959
C	-1.05449	1.546561	-0.22604
S	-3.42403	0.340762	-0.31027
C	-4.04294	-1.33359	0.033205
C	2.515708	0.600791	0.62972
C	3.32141	-0.40152	-0.2041
O	2.874233	-1.39263	-0.71684
O	4.604974	-0.02467	-0.25636
H	-1.50111	-1.76427	0.623363

H	0.909779	-1.58646	0.968207
H	0.814957	2.565607	-0.1975
H	-1.61122	2.413144	-0.56404
H	-5.11115	-1.28772	-0.17669
H	-3.88663	-1.59041	1.080885
H	-3.56997	-2.05735	-0.63051
H	2.753736	0.378639	1.679256
H	2.887179	1.607245	0.436218
H	5.104992	-0.68688	-0.76113

Table S20. XYZ coordinate of MTBa by B3LYP/6-311+G(d,p).

	X	Y	Z
C	-0.10985	-0.22985	0.000006
C	0.835715	-1.26656	-1E-06
C	2.194874	-0.97759	-6E-06
C	2.638122	0.346284	-3E-06
C	1.701801	1.375442	0.000003
C	0.334312	1.096111	0.000006
S	-1.82419	-0.71994	0.000004
C	-2.72519	0.861513	-9E-06
H	0.502245	-2.29872	-1E-06
H	2.911572	-1.79139	-0.00001
H	3.69856	0.569229	-6E-06
H	2.029934	2.409182	0.000003
H	-0.37022	1.917213	0.000008
H	-3.78139	0.59063	-0.00002
H	-2.5112	1.445406	0.896094
H	-2.51118	1.445404	-0.89611

Table S21. XYZ coordinate of MTBb by B3LYP/6-311+G(d,p).

	X	Y	Z
C	0.123257	-2E-06	-0.27115
C	-0.57037	-1.20816	-0.14835
C	-1.94055	-1.20631	0.108223
C	-2.62705	0.000002	0.238641
C	-1.94055	1.206312	0.10822
C	-0.57037	1.208161	-0.14835
S	1.885493	-3E-06	-0.63626
C	2.579555	0.000004	1.062776
H	-0.03512	-2.14369	-0.26088
H	-2.47134	-2.14731	0.201115
H	-3.69329	0.000003	0.435016
H	-2.47133	2.147308	0.201111
H	-0.03512	2.14369	-0.26089
H	3.664758	0.000006	0.950101
H	2.274987	0.893989	1.607264
H	2.274991	-0.89398	1.60727

Table S22. XYZ coordinate of MTBc$^{\bullet+}$ by UB3LYP/6-311+G(d,p).

	X	Y	Z
C	-0.11633	-0.21049	-1E-06
C	0.831451	-1.2791	0
C	2.179536	-0.9939	0
C	2.610096	0.342169	0
C	1.679036	1.400605	0
C	0.326766	1.138411	-1E-06

S	-1.76275	-0.70657	-1E-06
C	-2.76822	0.806726	0.000001
H	0.483597	-2.3059	0.000002
H	2.903788	-1.79875	0.000001
H	3.670713	0.564832	0.000001
H	2.030073	2.425183	0
H	-0.3824	1.954768	-1E-06
H	-3.8009	0.459014	0.000008
H	-2.57745	1.389752	0.901179
H	-2.57746	1.389747	-0.90118

Table S23. XYZ coordinate of MTTa by B3LYP/6-311+G(d,p).

	X	Y	Z
C	0.60315	-0.26325	-6E-06
C	0.063151	1.023687	-1.5E-05
C	-1.32203	1.204284	-1.1E-05
C	-2.20289	0.123677	0.000001
C	-1.64657	-1.16345	0.00001
C	-0.27293	-1.35945	0.000007
S	2.348071	-0.63431	-1.6E-05
C	3.133891	1.007277	0.000029
C	-3.69943	0.320988	0.000006
H	0.703609	1.895932	-2.7E-05
H	-1.71674	2.215538	-1.7E-05
H	-2.30125	-2.02969	0.00002
H	0.126421	-2.36811	0.000018
H	4.206943	0.813569	0.000043
H	2.878035	1.574497	0.89596

H	2.878067	1.574534	-0.89589
H	-3.95946	1.381535	-9E-06
H	-4.16144	-0.13566	0.881069
H	-4.16145	-0.13569	-0.88104

Table S24. XYZ coordinate of MTTb by B3LYP/6-311+G(d,p).

	X	Y	Z
C	0.612286	-3E-06	-0.30237
C	-0.09264	1.203901	-0.21675
C	-1.4734	1.199222	-0.03335
C	-2.1871	0.000001	0.066051
C	-1.4734	-1.19922	-0.03334
C	-0.09264	-1.20391	-0.21674
S	2.389227	-7E-06	-0.57755
C	2.999695	0.000012	1.1534
C	-3.67925	0.000004	0.29306
H	0.441831	2.142757	-0.30403
H	-2.00445	2.144121	0.025902
H	-2.00445	-2.14412	0.025921
H	0.441825	-2.14276	-0.30401
H	4.089235	0.000011	1.094795
H	2.668435	-0.89384	1.682404
H	2.668435	0.893877	1.682384
H	-4.14909	0.884516	-0.14308
H	-3.91169	0.000023	1.363752
H	-4.14909	-0.88453	-0.14305

Table S25. XYZ coordinate of MTTc$^{\bullet+}$ by UB3LYP/6-311+G(d,p).

	X	Y	Z

C	0.605424	-0.24787	-0.00127
C	0.060711	1.063276	-0.00517
C	-1.30309	1.228879	-0.0112
C	-2.18612	0.116438	-0.01154
C	-1.63159	-1.18496	-0.00891
C	-0.27118	-1.37437	-0.00311
S	2.282894	-0.62371	0.004403
C	3.169752	0.963634	0.003803
C	-3.66325	0.323265	0.010479
H	0.706836	1.930549	-0.00638
H	-1.71817	2.23021	-0.01729
H	-2.29154	-2.04429	-0.01363
H	0.143254	-2.37621	-0.00246
H	4.225878	0.695559	0.007707
H	2.934656	1.532969	0.902935
H	2.940208	1.529034	-0.89923
H	-3.95393	1.211971	-0.55368
H	-3.99466	0.483089	1.046107
H	-4.20277	-0.54327	-0.37299

Table S26. XYZ coordinate of MTAa by B3LYP/6-311+G(d,p).

	X	Y	Z
C	-1.03336	0.299223	-5E-06
C	-0.29105	1.492697	0.000009
C	1.09222	1.468917	0.000009
C	1.781199	0.248446	-2E-06
C	1.05615	-0.94114	-7E-06
C	-0.34368	-0.91061	-1.2E-05

S	-2.81195	0.46252	-1.5E-05
C	-3.39436	-1.26116	0.000024
O	3.145732	0.333256	0.000005
C	3.897041	-0.87138	-1E-06
H	-0.80599	2.447348	0.000019
H	1.663934	2.389222	0.00002
H	1.555181	-1.90102	-5E-06
H	-0.87506	-1.85326	-1.8E-05
H	-4.48298	-1.1989	0.000029
H	-3.072	-1.79372	-0.89595
H	-3.07199	-1.79368	0.896012
H	4.943491	-0.57048	-8E-06
H	3.692932	-1.47094	0.894277
H	3.692916	-1.47093	-0.89428

Table S27. XYZ coordinate of MTAb by B3LYP/6-311+G(d,p).

	X	Y	Z
C	1.027514	-0.01319	-0.30916
C	0.206695	1.112853	-0.26255
C	-1.17536	0.992677	-0.10323
C	-1.74977	-0.27609	0.010313
C	-0.93355	-1.41373	-0.04286
C	0.436702	-1.28095	-0.20507
S	2.797585	0.156978	-0.55533
C	3.394004	0.133722	1.180546
O	-3.08307	-0.51018	0.168869
C	-3.96969	0.600145	0.220639
H	0.64806	2.098162	-0.3566

H	-1.78303	1.887063	-0.07327
H	-1.39726	-2.38963	0.037173
H	1.059999	-2.16587	-0.25974
H	4.480049	0.229206	1.134181
H	2.982863	0.971915	1.743622
H	3.137585	-0.80728	1.667802
H	-4.96538	0.178881	0.348284
H	-3.74138	1.254418	1.068869
H	-3.93764	1.180282	-0.7078

Table S28. XYZ coordinate of MTAc$^{\bullet+}$ by UB3LYP/6-311+G(d,p).

	X	Y	Z
C	-1.03503	0.287295	0.000002
C	-0.29128	1.50679	0.000003
C	1.07347	1.483452	0.000002
C	1.765739	0.239717	-2E-06
C	1.035135	-0.97813	0.000005
C	-0.33866	-0.94968	0.000004
S	-2.74863	0.458498	-2E-06
C	-3.42898	-1.22936	-3E-06
O	3.079917	0.324023	-7E-06
C	3.918766	-0.85588	-1E-06
H	-0.81735	2.454484	0.000005
H	1.657158	2.395332	0.000004
H	1.549807	-1.9291	0.000012
H	-0.88201	-1.8848	0.000004
H	-4.51023	-1.09401	-5E-06
H	-3.13245	-1.76503	-0.90139

H	-3.13245	-1.76503	0.901387
H	4.935801	-0.47542	-9E-06
H	3.737756	-1.44489	0.900487
H	3.737751	-1.44491	-0.90048

Table S29. XYZ coordinate of $MTAd^{\bullet+}$ by UB3LYP/6-311+G(d,p).

	X	Y	Z
C	1.013784	-0.23335	0.000014
C	0.066397	-1.29973	0.000021
C	-1.28153	-1.04661	0.000015
C	-1.73669	0.29671	0.000001
C	-0.7957	1.366369	0.00002
C	0.548078	1.108877	0.000023
S	2.668488	-0.71217	-0.00001
C	3.638384	0.827343	-2.1E-05
O	-3.00209	0.662194	-1.4E-05
C	-4.07246	-0.31297	-2.3E-05
H	0.419328	-2.32483	0.000035
H	-1.98232	-1.86982	0.000021
H	-1.17728	2.379844	0.00003
H	1.245594	1.935111	0.000033
H	4.678519	0.502639	-4.3E-05
H	3.44025	1.407153	-0.90114
H	3.440289	1.407147	0.901113
H	-4.98575	0.274355	-2.5E-05
H	-4.01966	-0.92717	-0.90031
H	-4.01967	-0.92719	0.90026